Elsevier Editorial(tm) for Advances in Space Research
Manuscript Draft

Manuscript Number:

Title: Title of Manuscript: METHOD FOR CALCULATING GRAVITY WAVE ENERGY AND MOMENTUM FLUX FROM SATELLITE OBSERVATION

COSPAR Paper Number from Final Programme: C2.1-0051-04

Article Type: Contributed Paper

Keywords: Atmospheric Dynamics; Gravity Wave; Stratosphere; Mesosphere; Satellite Observation; Diffusive Spectrum Model

Corresponding Author: Dr. Jonathan H. Jiang California Institute of Technology

Other Authors: Ding-Yi Wang, Ph.D., M.Sc., B.Sc. IMK, Germany

Advances in Space Research, C2.1-0051-04, COSPAR- 2004

METHOD FOR CALCULATING GRAVITY WAVE ENERGY AND MOMENTUM FLUX FROM SATELLITE OBSERVATION

Jonathan H. Jiang[1] and Ding-Yi Wang[2]

[1]*Jet Propulsion Laboratory, California Institute of Technology, Pasadena, California 91109, USA*
[2] *Forschungszentrum Karlsruhe GmbH und Universität Karlsruhe, Institut für Meteorologie und Klimaforschung (IMK), Karlsruhe, Germany*

ABSTRACT

We present a semi-empirical method to compute gravity wave energy, momentum flux and wave drag using satellite temperature or radiance temperature variance measurements. Examples of using this method are demonstrated by using data from UARS MLS to estimate total wave energy, momentum flux and wave-induced mean-flow acceleration in the stratosphere and mesosphere associated with orographic and convective gravity waves. The method can be used in a number of current and future satellite experiments to improve the understanding of global gravity wave properties and their impact on the processes in the middle atmosphere.

INTRODUCTION

Atmospheric gravity waves often consist of a broad spectrum of spatial scales and temporal frequencies. In contrast, restrictions are imposed on the wave spectrum observed from satellite due to instrument limitations and sampling scenarios. For example, for the radiance variance data that are used in this study, the Microwave Limb Sounder (MLS) instrument on board the Upper Atmosphere Research Satellite (UARS) filters out most waves of horizontal scales greater than ~100 km and vertical scales smaller than ~10 km. If we have knowledge about the spectrum of the satellite-observed gravity waves, the wave associated total energy can be estimated, and the wave-induced momentum flux and wave drag can be inferred. In the lack of information on the actually measured spectrum, one can assume a model spectrum in view of the universality of gravity wave spectrum [*VanZandt*, 1982; 1985].

This study outlines a semi-empirical parameterization scheme, based on the diffusive spectrum model of *Gardner* [1994] (G94, hereafter), and uses this model to estimate information on the wave energy, momentum flux and drag from satellite data. Initial results from UARS MLS are given followed by the conclusion.

PARAMETERIZATION BASED ON DIFFUSIVE SPECTRUM MODEL

The G94 diffusive spectrum model imposes a cut-off vertical wave number, beyond which the waves are assumed to be removed from the spectrum by diffusion and/or critical layer interactions. Several comparisons between the model predictions and observational results have been conducted for the vertical wave number spectrum of simultaneous Na and Rayleigh lidar measurements in the stratosphere (25-45 km) and upper mesosphere (80-105 km) at Arecibo [*Beatty et al*., 1992; and *Senft et al*.. 1993], and for the vertical and horizontal wave number spectra of WINDII (The Wind Imaging Interferometer) green line wind and temperature at 87-110 km [*Wang et al*., 2000]. It turns out that the power law model, as an idealized description, provided a reasonable agreement with existing experimental data, although some deviations of the source spectrum from a pure power law behavior are reflected in the spectra observed at different geolocations and times.

Using the joint three-dimensional (k,l,m) diffusive model spectra in G94, we can find the ratio between the observed variance of fractional temperature perturbation $\overline{\langle (T'/T_0)^2 \rangle}$ and the total wave energy E_0 in the form of

$$R_T = \frac{\overline{\langle (T'/T_0)^2 \rangle}}{E_0} = \int_{h_c}^{m_d} \frac{1}{h} dh \int_{\substack{Eq\,3 \\ m \le m_c}} \frac{N^4}{g^2} \frac{\omega^2 - f^2}{\omega^2 (N^2 - \omega^2)} A(m) B(\omega) Q_u(\omega) \left| \frac{d\omega}{dh} \right| dm \qquad (1)$$

where k, l and m are the zonal, meridional, and vertical wave numbers and $h = (k^2 + l^2)^{1/2}$, N and f are the *Brunt – Väisälä* and inertial frequency, and g the gravitational acceleration. $A(m)$ and $B(\omega)$ are the normalized one-dimensional vertical wave number and frequency model spectra. $Q_u(\omega)$ is the appropriate polarization weighting term. The intrinsic wave frequency ω is determined from the gravity wave dispersion relation, with

$\omega = (N^2h^2 + f^2m^2)^{1/2}(m^2 + h^2)^{-1/2}$, and the Jacobian $|d\omega/dh| = (N^2 - f^2)hm^2(N^2h^2 + f^2m^2)^{-1/2}(m^2 + h^2)^{-3/2}$. As discussed below, diffusive damping set a limitation given by Equation (4) and $m = m_d$, where the spectrum falls to zero and all waves with $m > m_d$ are eliminated. Also, satellite instruments usually put limitations on the allowed wave numbers with $h \geq h_c$ and $m \leq m_c$.

The atmospheric diffusive effect also puts a limitation on the allowed wavenumbers and frequencies, i.e.

$$f \leq m^2 D(z) \leq \omega \leq N \,, \tag{2}$$

where $D(z)$ is the total effective diffusivity of the atmosphere, which is the sum of the eddy (including the wave and turbulence induced eddy diffusion) and molecular diffusivities. $D(z)$ varies with altitude z and may also depend on m and/or ω (see G94 and *Wang et al.*, [2000]). Its values can be taken from other existing models. In this analysis, we assume the dominance of wave-induced eddy diffusion and a simple analytical diffusivity model of G94 in the form of

$$D(z) = \overline{\langle (u')^2 \rangle} \frac{f}{N^2} \frac{\xi(p)}{2} = D_0 \exp\left[\frac{2z}{(s+3)H}\right] \tag{3}$$

where $D_0 \sim 2.573$ at mid-latitudes is the effective diffusivity at the ground $z = 0$.

The limit on the ω is understood as follows. In the absence of the diffusive effect, the temporal spectrum would cover the complete frequency range between f and N. However, the atmospheric diffusion distorts the ordered motions imposed on the atmosphere by the propagating wave and eventually leads to attenuation of the wave. The dissipations are most severe when the vertical diffusion velocity mD exceeds the vertical phase velocity ω/m. Since $D(z)$ increases with altitude, the wave spectrum is selectively filtered as the wave propagates upwards in the atmosphere with the long period, short vertical wavelength waves experiencing the most severe damping and being progressively removed from the spectrum. Only waves satisfying $mD \leq \omega/m$ are permitted to grow in amplitude with altitude. When the limitation of Equation (2) is applied to the joint three-dimensional (k,l,m) spectra, it can be converted into the form of

$$m_* \leq m \leq m_* L(m,h) \leq m_d \,, \tag{4}$$

where $L(m,h) = \left[(m/m_*)^2 + (h/h_*)^2\right]^{1/4}\left[(m/m_*)^2 + (h/h_*)^2(f/N)^2\right]^{-1/4}$, $m_d = m_*(N/f)^{1/2} = (N/D)^{1/2}$ and $m_* = (f/D)^{1/2}$.

The integral of Equation (1) can be numerically estimated for specified gravity wave model spectra. With $\overline{\langle (T'/T_0)^2 \rangle}$ obtained from the global measurements by the satellite-borne instruments, the total wave energy E_0 can be inferred. To estimate the momentum flux of gravity waves, we assume that fractions $0.5 - a$ and $0.5 + a$ of the wave kinetic energy are propagating along and against mean flow [*VanZandt and Fritts*, 1989]. The gravity wave spectrum observed in the summer mesopause region is highly anisotropic, with almost all wave motions propagating in the half plane opposed to the local mean flow, suggesting that $a \cong +0.5$ and that $\overline{u'w'}$ is against the mean flow [*Fritts and Wang* ,1991]. Near the tropopause, $a \cong +0.1$ has been inferred [*VanZandt and Fritts*, 1989]. The total momentum flux associated with the entire wave motion spectrum can be written as [*VanZandt and Fritts*, 1989 and G94]

$$\overline{u'w'} = -a \frac{1}{(2\pi)^2} \int_0^\infty dm \int_f^N d\omega F_u(m,\omega) \frac{\omega}{N} = -aE_0 \frac{f}{N} \xi(p) \tag{5}$$

where $F_u(m,\omega)$ is the two-dimensional horizontal velocity spectrum and $\xi(p)$ is a function of the spectral index (negative logarithmic slope) with $p \approx 2$ for the one-dimensional frequency spectrum. Here we have kept the non-diffusive form of Equation (5). Its diffusive version can be developed by imposing the conditions of (2) and (4). The induced mean flow acceleration, or wave drag can be estimated [*Fritts*, 1984] by

$$\overline{u_t} = \frac{\overline{u'w'}}{H} \,, \tag{6}$$

where subscript t denotes the time derivative, and H the atmospheric scale height.

SAMPLE RESULTS FROM UARS MLS

In this section, we demonstrate some initial results of computed wave energy, momentum flux and wave drag inferred from UARS MLS measurements. The fractional temperature perturbation in Equation (1) can be approximately related to the MLS normalized radiance variances $T_b'^2 / T_b^2$ as

$$\overline{\left\langle \left(T_b' / T_b\right)^2 \right\rangle} = \alpha \overline{\left\langle (T'/T_0)^2 \right\rangle}, \qquad (7)$$

where $\alpha \sim 0.2$ is estimated for the standard 4-point limb-scan and 6-point limb-track observations [*Jiang et al.*, 2004c]. The values of spectral slope *s* are computed by fitting with the MLS normalized radiances, yielding the vertical growth rates with scale heights of ~1.5 to ~2.5*H* [*Wu and Jiang*, 2002; *Jiang et al*. 2004a, 2004b]. With *s* determined, the total diffusivity *D* and critical wavenumber *m** can be inferred. The asymmetry factor $a = \pm 0.5$ is assumed in this preliminary analysis (sign '+' are used for westward fluxes and '–' for eastward fluxes). The instrument limitation can be determined as follows. Because of the UARS satellite motion (7.5 m/s) and MLS measurement time (2 sec), the MLS data filter out most waves of horizontal scales greater than ~60 km and 90 km, respectively for the 4-point limb-scan and 6-point limb-track data. MLS has eight combined-spectral-channels [*Jiang et al.* 2004a] featuring eight altitude layers at about 28, 33, 38, 43, 48, 53, 61, and 80 km. Due to smearing of the antenna field-of-view [*Wu and Waters*, 1996, 1997], the MLS data are limited to waves of vertical scales greater than ~10 km in the stratosphere and lower mesosphere (28-61 km) and ~ 15 km at altitude of 80 km. Therefore, $h \geq h_c = \sqrt{2} \cdot 2\pi/(60 \text{ or } 90 km)$ and $m \leq m_c = 2\pi/(10 \text{ or } 15 km)$ are used as the instrument limitation.

(1) Orographic waves

Recent work by *Jiang et al.* [2002, 2004a] using Mountain Wave Forecast Model (MWFM) simulation and MLS data analysis has shown that some large MLS wintertime radiance variance enhancements over mid- and high latitudes of both southern and northern hemispheres are orographic waves forced by flow over mountain ranges. We numerically programmed the diffusive spectrum model (described in section 1) to compute the MLS constrained total wave energy, momentum flux and wave induced mean flow acceleration (or wave drag) in the middle atmosphere. The results of three typical Arctic wintertime mountain waves are shown in Figure 1. The lower panel of Figure 1 shows the maps of total wave energy at 38 km height over mountainous regions of Scandinavia, Central Eurasia and Greenland. By applying the diffusive spectrum model, these wave energies are computed using the mean 6-point limb-track radiance variances [*Jiang et al*. 2004a] during December-February of 1994-1997, as acquired during MLS north-looking descending (ND) orbits. The momentum flux and wave drag profiles (Figure 1 top panel) are the mean values averaged for the latitude-longitude boxes that encircle the three mountainous regions (see figure caption). The MLS radiance variances measured from ND orbits are mostly sensitive to the gravity waves propagating westward. Thus the westward momentum fluxes are computed using the ND data. The eastward momentum fluxes are computed using the MLS north-looking ascending (NA) measurements, since the NA data are most sensitive to eastward propagating gravity waves. It can be seen that the magnitude of the MLS-inferred westward momentum fluxes are generally stronger then those associated with the eastward fluxes (see Figure 1 top-left panel). This momentum-flux asymmetry results a net westward wave-induced mean-flow acceleration (or wave drag) on the mostly eastward wintertime jets (see Figure 1 top-right panel). It has been noted that the presence of strong orographic wave activity in the stratospheric vortex and the net wave drag it produce could affect the middle atmospheric circulation and the temperature in the stratospheric vortex core [*Duck et al*., 2001].

Figure 1 also show a vertical growth of gravity wave momentum flux throughout the stratosphere until the stratopause altitude (~50 km). Above that level the wave strength decreases to about zero growth rate with height, possibly due to wave breaking or saturation at the stratopause [e.g. *Duck et al.*, 2001] and/or instrumental visibility effects [e.g. *Alexander*, 1998].

(1) *Convective waves*

The MLS observed summertime convective gravity waves are shown by *Jiang et al.* [2004b] and *McLandress et al*. 2000 to be mainly located in two monsoon regions (Indian and Central American) in northern summer (June-August) and three major subtropical convective centers (Southern Africa, Western Pacific, and South America) in southern summer (December-February). Applying the diffusive spectrum parameterization, we show in Figure 2 the computed the total wave energy, momentum flux and wave drag for the gravity waves centered in the three subtropical southern summer convective regions. The December-February 1991-1994 mean MLS 4-point limb-scan data measured from NA and south-looking descending (SD) are averaged to generated the total wave energy maps (Figure 2 lower panel). Study by *Jiang et al*. [2004b] found that convectively-generated stratospheric gravity waves

are mostly seen in the MLS NA and SD data, which are most sensitive to the eastward propagating waves in westward background winds. The westward convective waves, seen in the MLS south-looking ascending (SA) and ND data, are relatively weaker in strength. Thus, in contrary to the orographic waves, the magnitudes of the MLS-inferred westward momentum fluxes for convective waves are weaker than those associated with the eastward fluxes (Figure 2 top-left panel). This eastward momentum flux bias results a net eastward wave-induced mean-flow acceleration (or wave drag) on the mostly westward subtropical jet-stream. Compared to the mountain wave momentum flux profiles, the convective momentum flux profiles also show maxima at stratopause level but exhibit somewhat smaller gradient above.

CONCLUDING REMARKS

We have presented an overview of a semi-empirical diffusive spectrum model developed from the *Gardner's* [1994] spectral description of gravity wave-induced normalized radiance temperature variance. We have estimated gravity wave energy, momentum flux and wave drag using UARS MLS observations by applying this model with MLS instrument limitations. In the examples given above, momentum flux profiles above major Arctic winter mountainous regions and subtropical summer convection centers are computed. The maximum values of absolute gravity wave momentum fluxes are found to be up to ~20 $(m/s)^2$ for orographic waves and ~8 $(m/s)^2$ for convective waves at stratopause level. At stratosphere altitude ~38 km, the absolute total gravity wave energy is upto ~70 $(m/s)^2$ for orographic waves and ~45 $(m/s)^2$ for the convective waves, which corresponds to momentum fluxes ~2 $(m/s)^2$ and ~1 $(m/s)^2$, respectively. These values are in agreement to the momentum flux estimation from CRISTA (Cryogenic Infrared Spectrometers and Telescropes for the Atmosphere) observations, in which the typical momentum fluxes estimated from CRISTA data at 38 km over the subtropics and the southern Andes are about 0.36 to 1.3 $(m/s)^2$ [Preusse, Peter, personal communication, 2004]. Calculations by *Ern et al*., [2004] using CRISTA data show that the typical gravity wave momentum fluxes at 25 km are ~0.05 kg/m^3. Our analysis based on their 25 km altitude map finds their momentum flux corresponding to momentum flux values ranging from ~0.1 to ~1 $(m/s)^2$.

Some model uncertainties exist due to various assumptions made. The most important one is the value of asymmetry factor, which is assumed to be 0.5 in this preliminary study. In reality, it could be vary with time and geolocation in response to background mean flow due to Doppler-shifting effect on frequency spectra [e.g. *Fritts and Wang*, 1991]. Detailed knowledge on the asymmetry factor is to be developed by model calculation and experimental studies. In this aspect, simultaneous wind measurements are required to accurately quantify the Doppler effect. Further studies with ground based and satellite wind measurements will be preceded in the near future to determine the asymmetry factor. Nevertheless, we have shown that this semi-empirical model provides first order estimates of gravity wave energy, momentum flux and wave drag from UARS MLS measurements, and can be further extended for application to other satellite observations. For example, recently launched AIRS and AMSU instruments on Aqua satellite and the second generation MLS instrument on Aura satellite have been producing new higher resolution radiance temperature variance data for gravity wave studies. This semi-empirical model offers a useful tool which could help bridging gaps between the gravity wave theory and global observation in the middle atmosphere to improve our understanding of global gravity wave processes in the middle atmosphere.

ACKNOWLEDGMENTS

We thank Drs. Peter Preusse, Dave Fritts and Dong L. Wu for helpful comments and suggestions. This study was supported by the Jet Propulsion Laboratory, California Institute of technology, under contract with NASA. The authors also acknowledge the support of the Forschungszentrum Karlsruhe GmbH und Universität Karlsruhe, Institut für Meteorologie und Klimaforschung (IMK), Karlsruhe, Germany.

REFERENCES

Alexander, M. J., Interpretations of observed climatological patterns in stratospheric gravity wave variance, *J. Geophys. Res.*, 103, 8627-8640, 1998.

Andrwes, D. G., J. R. Holton, and C. B. Leovy, Middle Atmosphere Dynamics, Academic Press, San Diego Calif., 1987.

Beatty, T. J., C. A. Hosterler and C. S. Gardner, Lidar observations of gravity waves and their spectra near the mesopause and stratopause at Arecibo, *J. Atmos. Sci.*, 49,477-496, 1992.

Duck, T. J., J. A. Whiteway, and A. I. Carswell, The gravity wave-Arctic stratospheric vortex interaction, *J. Atmos. Sci.*, 58, 3581-3596, 2001.

Ern, M., P. Preusse, M.J. Alexander, and C.D. Warner, Absolute values of gravity wave momentum flux derived from satellite data, *J. Geophys. Res.*, in press, 2004.

Fritts, D. C., Gravity wave saturation in the middle atmosphere:A review of theory and observations, *Rev. Geophys. Space Phys.*, 22, 275, 1984.

Fritts, D. C., and D. Y. Wang, Doppler-shifting effects on frequency spectra of gravity waves observed near the summer mesopause at high latitude, *J. Atmos. Sci.*, 48,1535, 1991.

Gardner, C. S., Diffusive filtering theory of gravity wave spectra in the atmosphere, *J. Geophy. Res.*, 99, 20,601-20,622, 1994.

Jiang, J. H., D. L. Wu, S.D. Eckermann, Upper Atmosphere Research Satellite (UARS) MLS observation of mountain waves over the Andes, *J. Geophys. Res.* 107, D22, 10.1029 /2002JD002091, 2002.

Jiang, J.H, S.D. Eckermann, D.L. Wu, J. Ma, A Search for Mountain Waves in MLS Stratospheric Limb Radiances from the Winter Northern Hemisphere: Data Analysis and Global Mountain Wave Modeling, *J. Geophys. Res*. 109, No. D3, D03107, 10.1029/2003JD003974, 2004a.

Jiang, J.H, B. Wang, K. Goya, K. Hocke, S.D. Eckerman, J. Ma, D.L. Wu, W.G. Read, Geographical Distribution and Inter-Seasonal Variability of Tropical Deep Convection: UARS MLS Observations and Analyses, *J. Geophys. Res*. 109, D3, D03111, 10.1029/2003JD003756, 2004b.

Jiang, J.H., D.Y. Wang, D. Fritts, D. L. Wu, Seasonal Variation of MLS Measured Gravity Wave Energy, Momentum Flux and Wave Drag as Estimated from Diffusive Spectrum Model, *J. Amos. Sci*., to be submitted, 2004c.

McLandress, C., M. J. Alexander, and D. L. Wu, Microwave limb sounder observations of gravity waves in the stratosphere: a climatology and interpretation, *J. Geophys. Res*., 105, 11947-11967, 2000.

Senft, D. C., C. A. Hostetler, and C. S. Gardner, Characteristics of gravity wave activity and spectra in the upper stratosphere and upper mesosphere at Arecibo during early April 1989, *J. Atmos. Terr. Phys.*, 55, 425-439, 1993.

VanZandt, T. E., A universal spectrum of buoyancy waves in the atmosphere, *Geophys. Res. Lett.*, 9,575, 1982.

VanZandt, T. E., A model for gravity wave spectra observed by Doppler sounding system, *Radio Sci.*, 20,1323, 1985.

VanZandt, T. E., and D. C. Fritts, A theory of enhanced saturation of the gravity wave spectrum due to increase in atmospheric stability, *Pure Appl. Geophys.*, 130(2/3), 399, 1989.

Wang, D.Y., S. P. Zhang, R. H. Wiens, and G. G. Shepherd, Gravity waves from O2 nightglow during the AIDA '89 Campaign III: Effects of gravity wave saturation, *J. Atmos. Terr. Phys.*, 55, 397-408, 1993.

Wang, D. Y., W. E. Ward, B. H. Solheim, and G G. Shepherd, Wavenumber spectra of horizontal winds and temperature measured with WINDII, Part II: Diffusive effect on spectral formation, *J. Atmos. Solar-Terr. Phy.*, 62,981-991, 2000.

Wu, D. L., and J. W. Waters, Gravity-wave-scale temperature fluctuations seen by the UARS MLS, *Geophys. Res. Lett.*, 23, 3289-3292, 1996.

Wu, D. L., and J. W. Waters, Observations of gravity waves with the UARS Microwave Limb Sounder, *Gravity Wave Processes*, NATO ASI Series I: Global Environment Change, 50, 103-120, 1997.

Wu, D.L., J.H. Jiang, MLS Observations of Atmospheric Gravity Waves over Antarctica, *J. Geophys. Res.* 107, No. D24, 4773, 10.1029/2002JD002390, 2002.

Figure

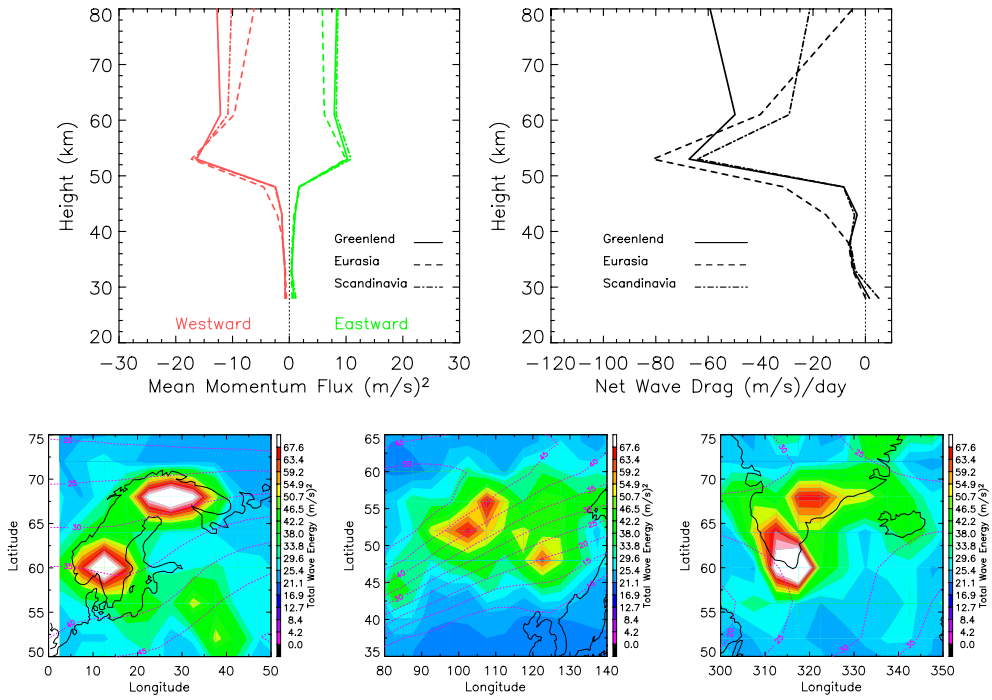

Figure 1: Lower panel: Total gravity wave energy $(m/s)^2$ at 38 km over mountainous regions of Scandinavia, Central Eurasia and Greenland, computed by applying the diffusive spectrum model using the 6-point limb-track normalized radiance variances during Dec-Feb of 1994-1997, as acquired during MLS ND orbits. Top-left panel: Mean gravity momentum flux $(m/s)^2$ profiles averaged for regions of Scandinavia (Lon: 4°-40°; Lat:: 57°N-72°N), Eurasia (Lon: 90°-130°; Lat: 45°N-60°N), and Greenland (Lon: 300°-335°; Lat: 55°N-70°N). The red lines are for the westward-propagating waves measured from MLS ND orbits; the green-lines are for the eastward-propagating waves measured from NA orbits. Top-right panel: The net wave-induced mean flow acceleration or wave drag ($ms^{-1}day^{-1}$) computed from the difference between the westward and the eastward momentum fluxes. The negative values of wave drag indicate a westward drag force. Both the momentum fluxes and wave drags are averaged values for the period of Dec-Feb of 1994-1997.

Figure

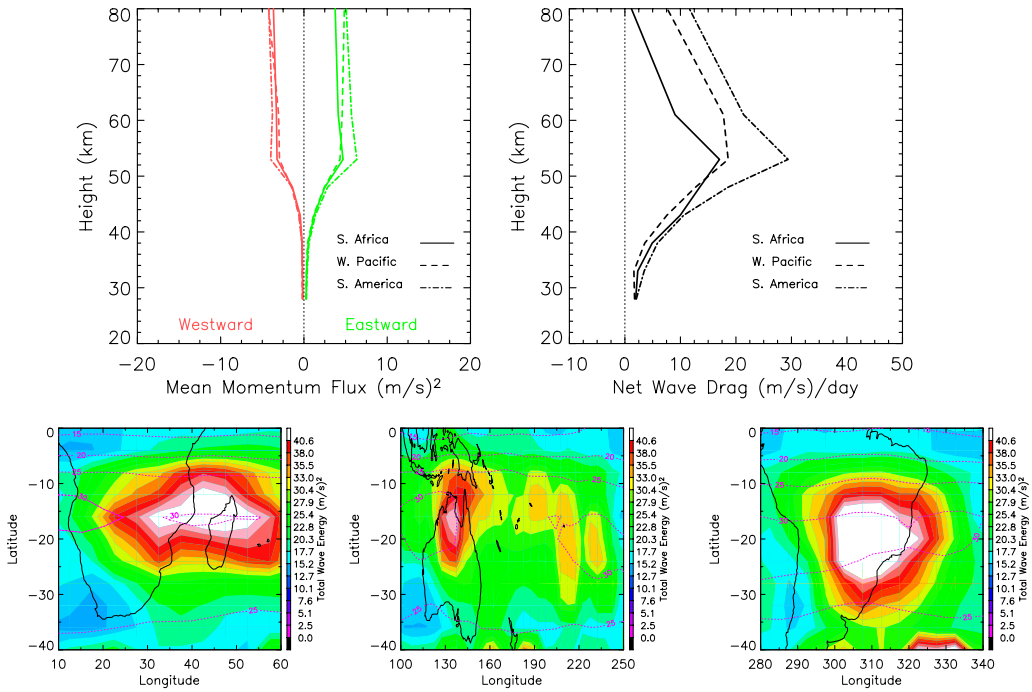

Figure 2: Lower panel: Total gravity wave energy $(m/s)^2$ at 38 km over convective regions of Southern Africa, Western Pacific and South America, computed by applying the diffusive spectrum model using the 4-point limb-scan normalized radiance variances during Dec-Feb of 1991-1994, as averaged using MLS NA and SD measurements. Top-left panel: Mean gravity momentum flux $(m/s)^2$ profiles averaged for regions of Southern Africa (Lon: 15°-60°; Lat:: 5°S-30°S), Western Pacific (Lon: 120°-240°; Lat: 5°S-30°S), and South America (Lon: 290°-330°; Lat: 5°S-35°S). The red lines are for the westward-propagating waves measured from MLS SA orbits; the green-lines are for the eastward-propagating waves measured from SD orbits. Top-right panel: The net wave-induced mean flow acceleration or wave drag ($ms^{-1}day^{-1}$) computed from the difference between the westward and the eastward momentum fluxes. The positive values of wave drag indicate a eastward drag force. Both the momentum fluxes and wave drags are averaged values for the period of Dec-Feb 1991-1994.